Mitochondrial Signs and Subcellular Imaging Provide Insight into the Antifungal Mechanism of Carabrone against *Gaeumannomyces graminis* var. *tritici*

Lanying Wang,[†,‡] Yunfei Zhang,[†] Delong Wang,[†] Mei Wang,[†] Yong Wang,[†] and Juntao Feng[*,†,#]

[†]Research and Development Center of Biorational Pesticide, Northwest A&F University, Yangling 712100, Shaanxi, China
[‡]Institute of Tropical Agriculture and Forestry, Hainan University, Haikou 570228, Hainan, China
[#]Engineering and Research Center of Biological Pesticide of Shaanxi Province, Yangling 712100, Shaanxi, China

Ⓢ *Supporting Information*

ABSTRACT: Carabrone, a botanical bicyclic sesquiterpenic lactone, has broad-spectrum antifungal activity and is particularly efficient against the devastating phytopathogen *Gaeumannomyces graminis* var. *tritici* (Ggt). The antifungal mechanism of carabrone against Ggt, however, remains unclear. The main objective of this study was to investigate the subcellular localization of carabrone in Ggt to gain a better understanding of its mechanism of action. When Ggt was exposed to carabrone (EC_{50} value of 28.45 μg/mL) for 7 days, a decline in mitochondrial concentration together with some obvious alternations in mitochondrial structure, including hazy outlines, medullary transitions, excess accumulation of unclear settlings, and vacuolar degeneration, were observed, indicating that carbrone may act on the mitochondria directly. A fluorescent conjugate (TTY) was thus designed and synthesized as a surrogate of carabrone that possessed comparable antifungal activity against Ggt (EC_{50} of 33.68 μg/mL). Additionally, a polyclonal antibody specific to carabrone and with a high titer (256 000) was also prepared by immunizing mice. Subsequently, two imaging techniques, the use of the fluorescent conjugate (FC) and immunofluorescence (IF), were applied to determine the subcellular localization of carabrone. Both FC and IF fluorescent signals demonstrated its mitochondrial localization with a Pearson's coefficient of 0.83 for FC and 0.86 for IF. These results imply that carabrone exerts its antifungal activity against Ggt by interfering with mitochondrial function.

KEYWORDS: carabrone, fluorescent conjugate, polyclonal antibody, immunofluorescence, subcellular localization, mitochondria, *Gaeumannomyces graminis* var. *tritici*

INTRODUCTION

Take-all, a worldwide soil-borne disease of wheat caused by *Gaeumannomyces graminis* var. *tritici* (Ggt), severely affects global wheat production and can bring about serious yield and economic losses in epidemic years.[1,2] The traditional control methods are often limited in practical application by the lack of resistant cultivars,[1,3] inefficiency of crop-rotation and tillage-management measures,[4] and poor robustness in take-all decline,[4] as well as environmental concerns and fungicide-resistance issues related to chemical fungicides.[5] Biocontrol agents[6] and botanical fungicides[7] have been recognized as safer and more effective alternatives to conventional strategies. To date, microorganisms such as pseudomonads[8,9] and *Bacillus* species[10,11] have been developed as biocontrol agents against take-all. However, natural chemical compounds effective against Ggt are rarely reported.[12]

Carabrone (Figure 1), a bicyclic sesquiterpenic lactone originally isolated from the fruit of *Carpesium abrotanoides*, is widely distributed in feverfew and other plant species[13] and exhibits diverse bioactive properties including antibacterial[14,15] and antitumor activities.[16] It has been reported that carabrone possesses broad-spectrum antifungal activity and that it was more effective against Ggt than against other phytopathogens tested, with an EC_{50} value of 28.45 μg/mL.[17] Although carabrone has great potential to be developed as an effective

antifungal agent for take-all control, the antifungal mechanism of carabrone against Ggt still remains unclear.

A vast array of sesquiterpene lactones depend on α-methylene-γ-butyrolactone structural motifs to exert their biological activities, and the motif may play a pivotal role in mediating interactions with unidentified target molecules.[18,19] In addition, a range of natural lactones, such as britannin,[20] arucanolide,[21] parthenolide,[22] costunolide,[23] and isocostunolide[24] have been proved to be involved in intracellular mitochondria-related pathways that induce apoptosis in cancer cells (Figure 1). Given its identical α-methylene-γ-butyrolactone substructure, we speculated that carabrone might also exert its antifungal activity against Ggt via targeting the mitochondria (Figure 1). Our previous studies also indicated that carabrone inhibited not only the intracellular oxidation process but also the activities of respiratory chain complexes I–V in Ggt.[25,26] Nonetheless, direct evidence supporting this hypothesis is still lacking.

Imaging techniques such as immunofluorescence (IF)[27,28] and synthesis of fluorescent conjugates (FC)[29,30] are widely used to investigate the subcellular distributions of bioactive
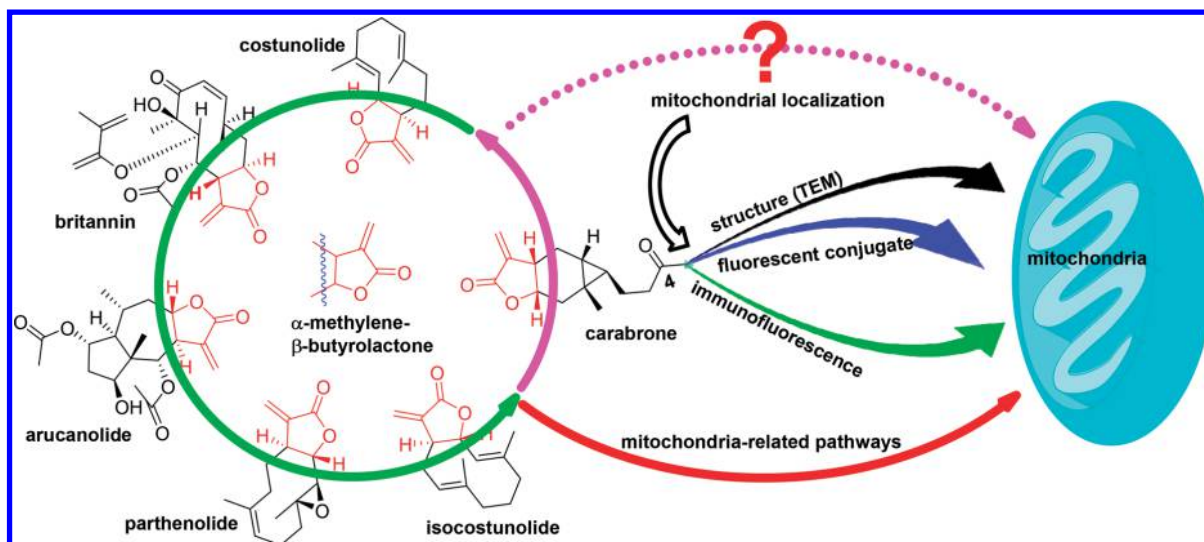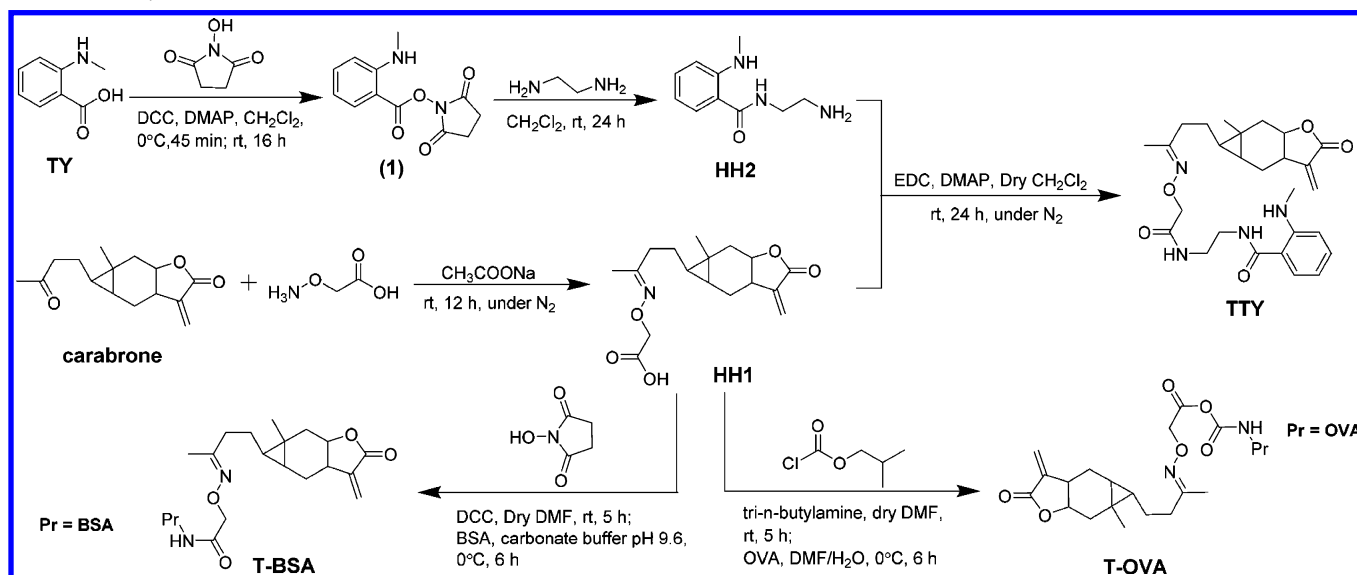
Figure 1. Hypothesis and research techniques used in this study of the mitochondrial localization of carabrone in Ggt.

Scheme 1. Synthesis of TTY, T-BSA, and T-OVA

molecules with high spatial and temporal resolution, and the action mechanisms of the corresponding molecules can be inferred on the basis of these techniques.[31−33] In order to verify our hypothesis (Figure 1), proposed above, we first examined the changes in mitochondrial ultrastructure and concentrations in Ggt hyphae exposed to carabrone. Subsequently, we designed and synthesized a fluorescently labeled carabrone analog, TTY, and generated a polyclonal antibody against carabrone. After investigating their properties and suitabilities for cell imaging, they were used to image the subcellular localization of carabrone in Ggt by the IF and FC techniques.

MATERIALS AND METHODS

General Information. The carabrone compound characterized in this study was isolated from *Carpesium macrocephalum* and purified (>98% in purity) in our laboratory. The NMR spectra were recorded on a Bruker AVANCE III 500 spectrometer (Rheinstetten, Germany) with tetramethylsilane as the internal standard. The mass spectra (MS) of the new compounds were obtained by a LCQ Fleet mass spectrometer (Waltham, MA). *N*-Methyl anthranilic acid (NAA, 98%), carboxymethoxylamine hemihydrochloride (99%), *N*-hydrox-

ysuccinimide (NHS, 98%), ethylenediamine (99%), 4-dimethylaminopyridine (DMAP, 98%), *N,N*-Dicyclohexylcarbodiimide (DCC, 97%), 1-(3-(dimethylamino)propyl)-3-ethylcarbodiimide hydrochloride (EDC, 98%), isobutyl chloroformate (98%), tributylamine (97%), and tetramethylbenzidine (TMB, 98%) were purchased from Aladdin Company Ltd. (Shanghai, China). Bovine albumin (BSA), ovalbumin (OVA), incomplete Freund's adjuvant (IFA), complete Freund's adjuvant (CFA), tween-20, tritonX-100, parafomaldehyde, HRP-labeled goat anti-mouse-IgG (H+L) antibodies, anti-mouse IgG (whole molecule)-FITC antibodies, cellulase, Driselase, and lyticase were purchased from Sigma-Aldrich (St. Louis, MO). MitoTrackerR Green FM (M7514), and MitoTrackerR Red CMXRos (M7512) were purchased from Invitrogen (Waltham, MA). RedDot1 (200×) was obtained from Biotium (Fremont, CA). All organic solvents were commercial AR solvents and were purified when necessary. The silica gels for TLC and column chromatography were obtained from Qingdao Haiyang Chemical Company Ltd. (Qingdao, China).

Synthesis of Fluorescently Labeled Carabrone (TTY). 2-(((4-(5a-Methyl-3-methylene-2-oxooctahydro-2H-cyclopropa[f]-benzofuran-5-yl)butan-2-ylidene)amino)oxy)acetic Acid (HH1). HH1 was prepared according to the reported method[34] with some modifications. Briefly, carboxymethoxylamine hydrochloride (196.82 mg, 2.4 mmol, 1.2 equiv) and sodium acetate (1.2 equiv) were

successively added to a solution of carabrone (1.0 equiv) in 20 mL of 95% ethanol. The reaction mixture was stirred at room temperature under nitrogen for 12 h. After that, the resultant mixture was filtered, evaporated, and purified by column chromatography on a silica gel (80−100 mesh) using petroleum ether/ethyl acetate/acetic acid (2/1/0.05, v/v/v) as the eluate to yield HH1, a colorless oil (yield of 90.3%). ^{1}H NMR (500 MHz, CD$_3$OD) δ 6.17 (d, J = 2.0 Hz, 1H), 5.68 (d, J = 2.0 Hz, 1H), 4.53 (d, J = 11.5 Hz, 2H), 3.30−3.19 (m, 1H), 2.50 (t, J = 7.6 Hz, 1H), 2.45−2.35 (m, 1H), 2.24−2.32 (m, 3H), 1.90 (d, J = 25.2 Hz, 3H), 1.66−1.56 (m, 1H), 1.51 (dq, J = 14.8, 7.5 Hz, 1H), 1.12 (dd, J = 10.8, 5.6 Hz, 4H), 0.99 (m, 2H), 0.62−0.52 (m, 1H), 0.51−0.39 (m, 1H); ^{13}C NMR (125 MHz, MeOD) δ 171.31, 159.94, 159.44, 139.72, 121.69, 76.33, 69.43, 37.61, 36.82, 35.03, 33.95, 30.36, 25.60, 22.97, 16.55, 13.15; ESI-MS, m/z 322.2 [M + H]$^+$.

N-(2-(2-(((4-(5a-Methyl-3-methylene-2-oxooctahydro-2*H*-cyclopropa[f] benzofuran-5-yl)butan-2-ylidene)amino)oxy)-acetamido)ethyl)-2-(methylamino)benzamide (TTY).* The synthesis procedures of TTY were modified according to the literature.[35,36] *N*-Methyl anthranilic acid (TY, 302.3 mg, 2 mmol, 1 equiv) was dissolved in 20 mL of dry CH$_2$Cl$_2$, to which NSH (1.5 equiv) and a catalytic amount of DMAP (0.1 equiv) were added. After the mixture was cooled to 0 °C, a solution of DCC (1.5 equiv) in 10 mL of anhydrous CH$_2$Cl$_2$ was added dropwise into the mixture. The reaction mixture was stirred at 0 °C for 45 min and then stirred at room temperature for another 16 h. The mixture was filtered and the filtrate was washed with 0.05 N HCl (2 × 10 mL) and brine. The organic layer was dried over anhydrous Na$_2$SO$_4$, filtered, and evaporated by a rotary evaporator to yield **1** (Scheme 1). The obtained compound, **1**, was dissolved in 20 mL of dry CH$_2$Cl$_2$, and the resulting solution was added dropwise to 10 mL of anhydrous CH$_2$Cl$_2$ with 41.33 mmol of ethylenediamine (2.75 mL) over 30 min. The mixture was stirred at room temperature under nitrogen for 24 h and then filtered and washed with brine (3 × 100 mL). The organic layer was dried over anhydrous Na$_2$SO$_4$, filtered, concentrated, and purified by chromatography on a silica gel (80−100 mesh) using dichloromethane/ethanol/ammonium hydroxide (30/1/0.05, v/v/v) as the eluate to yield HH2. HH1 (250 mg, 0.78 mmol, 1 equiv), EDC (1.2 equiv), and DMAP (0.1 equiv) were dissolved in anhydrous CH$_2$Cl$_2$ (30 mL) and stirred at 0 °C for 30 min. Then, a solution of HH2 (1.5 equiv) in anhydrous CH$_2$Cl$_2$ (10 mL) was added dropwise to the mixture within 30 min. The reaction mixture was stirred at room temperature for another 24 h and then filtered, concentrated, and purified by chromatography on a silica gel (80−100 mesh). Elution with petroleum ether/ethyl acetate/ammonium hydroxide (1/5/0.05, v/v/v) gave the pure compound TTY, a slightly yellow oil (yield of 61.7%). The fluorescent properties of compound TTY in vitro were monitored using an F-4500 fluorescence spectrophotometer (Hitachi, Tokyo, Japan) with a scanning mode of 250−400 nm for the excitation spectrum and 415−800 nm for the emission spectrum. ^{1}H NMR (500 MHz, CDCl$_3$) δ 7.56 (s, 1H), 7.41 (dd, J = 7.8, 1.1 Hz, 1H), 7.33 (t, J = 7.8 Hz, 1H), 7.29 (s, 1H), 7.28 (s, 1H), 6.67 (d, J = 8.4 Hz, 1H), 6.61 (t, J = 7.5 Hz, 1H), 6.25 (d, J = 2.3 Hz, 1H), 5.57 (d, J = 2.3 Hz, 1H), 4.85−4.69 (m, 1H), 4.52 (s, 2H), 3.56 (s, 3H), 3.16 (dt, J = 11.6, 9.0 Hz, 1H), 2.87 (s, 3H), 2.32 (ddd, J = 20.1, 13.9, 6.4 Hz, 2H), 2.25−2.18 (m, 2H), 1.93 (s, 3H), 1.54 (dt, J = 14.3, 7.1 Hz, 1H), 1.48−1.37 (m, 1H), 1.28 (t, J = 7.1 Hz, 1H), 1.07 (s, 3H), 1.05−0.88 (m, 2H), 0.41 (dt, J = 11.2, 5.7 Hz, 1H), 0.38−0.32 (m, 1H); ^{13}C NMR (125 MHz, CDCl$_3$) δ 171.69, 170.72, 170.63, 160.08, 150.60, 139.09, 132.98, 127.59, 122.72, 114.69, 114.46, 111.04, 75.72, 72.45, 40.26, 39.59, 37.52, 37.10, 35.64, 33.89, 30.61, 29.68, 25.87, 22.83, 18.36, 17.09, 14.56; ESI-MS, m/z 497.3 [M + H]$^+$.

Preparation of Immunogen and the Coating Antigen. Immunogen (T-BSA) was synthesized according to the method described by Wang et al. with slight modifications.[37] Hapten (HH1, 15.6 mg, 0.048 mmol) was dissolved in 1.0 mL of dry DMF containing 0.28 mmol of NSH. The mixture was stirred for 15 min at room temperature, and 0.20 mmol of DCC was added. After stirring in the dark for 5 h, the reaction mixture was centrifuged (10 000 rpm, 10 min, 4 °C) to remove the precipitate. The resulting supernatant was added slowly to 5 mL of carbonate buffer (50 mM, pH 9.6) with 50

mg of BSA under magnetic stirring at 0 °C within 30 min. After that, the reaction continued for 6 h under the same conditions and was purified by dialyzing it extensively with phosphate-buffered saline (PBS, 10 mM, pH 7.4) for 3 days at 4 °C. The purified T-BSA solution was lyophilized and kept at −20 °C for later use.

The preparation of the coating antigen (T-OVA) was performed according to Gendloff et al.'s method[38] with some revisions. Briefly, 15.6 mg of HH1 was dissolved in 1 mL of dry DMF and cooled to 0 °C. To this, 77 μL of tri-*n*-butylamine and 22 μL of isobutyl chloroformate were added, and the mixture was stirred at room temperature for 5 h. After cooling to 0 °C, the mixture was added dropwise to a stirring mixture solution of DMF/water (10 mL, 1/4, v/v) containing 88 mg of OVA within 30 min. Under constant conditions, the reaction was maintained for another 6 h. The subsequent procedures were identical to those of T-BSA, described above.

The hapten-protein conjugates, T-BSA and T-OVA, were characterized by SDS-PAGE and by their UV spectra. SDS-PAGE analysis of the conjugates was performed by using a 3% stacking gel and a 10% separating gel and Coomassie Blue staining. UV spectra were obtained by spectral scanning (240−320 nm) of the proteins and their conjugates with a UV-3310 spectrophotometer (Hitachi, Tokyo, Japan).

Preparation of the Polyclonal Antibody. Female BALB/c mice were obtained from the Experimental Animal Research Center, Fourth Military Medical University (Shaanxi, China) and had an average body weight of 20 g. They were housed under standard laboratory conditions with free access to drinking water and a commercial pellet diet. Animal manipulations were carried out in compliance with the Animal Management Rules of the Ministry of Health of China (No. 55, 2001). Six female BALB/c mice of 6 weeks of age were immunized with the antigen following the immunizing protocol described by Leenaars and Hendriksen.[39] Before immunization, blood was collected by tail bleeding to prepare control serums. Initial immunization was carried out by multiple subcutaneous injections with an emulsion of a physiological brine solution containing 50 μg of T-BSA and complete Freund's adjuvant (1/1, v/v) for each mouse. Two weeks later, each mouse was boosted with 50 μg of T-BSA in incomplete Freund's adjuvant two times at 1 week intervals. One week after the third inoculation, each mouse was given a single intraperitoneal injection with 100 μg of T-BSA in a physiological brine solution. After 1 week, blood samples were harvested by removing the eyeballs, and titers of the antisera were monitored by indirect enzyme-linked immunosorbent assays (ELISAs) as described by Manclús and Montoya[40] to evaluate the immune responses. The antiserum with highest titer was purified by affinity column chromatography on a Sepharose-4B gel to prepare the polyclonal antibody. Antiserum titer was defined as the reciprocal of the highest dilution that gave an absorbance of about 1.0. The concentration of the purified polyclonal antibody was measured using a NanoVue Plus at 280 nm, and the sample was stored at −20 °C for further use.

Antifungal Bioassay. The antifungal activity of TTY against Ggt was determined by the agar dilution method described by Rios et al.[41] Stocks of carabrone and TTY in DMSO with different concentrations were prepared in advance. Stock solutions (50 μL) were added to molten PDA (50 mL) at low temperatures (45−50 °C). After sufficient mixing, the solutions were poured immediately into 90 mm Petri dishes to a thickness of 2−3 mm, resulting in dishes with different concentrations of carabrone or TTY (6.25, 12.50, 25.00, 50.00, or 100.00 μg/mL). PDA supplemented with DMSO served as the control. After plating, a 4 mm diameter mycelial disc from the actively growing colony front was then aseptically placed with the inoculum-side down in the center of each treatment plate. The plates were then incubated in the dark at a constant temperature of 25 °C for 7 days. All experiments were conducted in a sterile environment and performed in triplicate. The mean growth values were measured and subsequently converted into an inhibition rates of mycelial growth in relation to the control treatment according to the following formula:

$$\text{inhibition rate (\%)} = [(M_c - M_t)(M_c - 0.4)] \times 100\%$$

where M_c and M_t represent the mycelial growth diameters of the control and treatment groups, respectively. The EC_{50} values (effective dose for 50% inhibition) were calculated statistically by probit analysis using the probit package of the SPSS 23.0 software (SPSS Inc., New York, NY).

Effects of Carabrone on Hyphal Morphology and Ultrastructure. The effects of carabrone on hyphal morphology and ultrastructure were investigated using the reported method of Shao et al.[42] A prepared mycelial agar disc from a 5-day-old culture was inoculated in the center of a PDA plate with the EC_{50} value of carabrone (28.45 μg/mL) and incubated at 25 °C for 7 days in the dark. PDA plates without carabrone treatments were used as the controls.

For the scanning electron microscope (SEM) observations, mycelial discs ($3 \times 5 \times 5$ mm) were fixed with 2.5% glutaraldehyde in 0.1 M phosphate buffer (pH 7.2) overnight at 4 °C. After fixation, the mycelial discs were gently washed with 0.1 M phosphate buffer (pH 7.2) six times (15 min each). Then, the fixed samples were dehydrated in a graded ethanol series (once at 30, 50, 70, 80, and 90% and three times at 100%, v/v, 15 min each). After the dehydration period, each specimen was dipped into pure isoamyl acetate for replacement two times (30 min each). Finally, the samples were dried by supercritical carbon dioxide, gold-coated by an E1010 sputter coating machine (Hitachi, Tokyo, Japan) for 60 s, and then imaged using a JSM-6360LV SEM (JEOL, Tokyo, Japan). The untreated mycelial discs were used as the controls.

For the transmission electron microscopy (TEM) observations, the fixed mycelia for the SEM observations were postfixed with 1% osmic acid for 2 h. Then, the samples were fully washed with 0.1 M phosphate buffer (pH 7.2), which was immediately followed by dehydration of the samples as described above. The samples were dipped into epoxy propane two times (15 min each). After that, the specimens were passed through the solution of epoxy resin and epoxy propane (1:1, v/v) for 1 h and embedded in epoxy media at 55 °C for 48 h. The ultrathin sections were prepared with a Ultramicrotome (Leica-ULTRACUT, Wetzlar, Germany), contrasted with 2% uranyl acetate followed by 2% lead citrate, and examined on a JEM-1230 TEM (Hitachi, Tokyo, Japan). Each microscopy technique, TEM and SEM, was used to examine at least three samples from each of the treated and control groups.

Effect of Carabrone on Mitochondrial Concentration. The extraction of mitochondria was performed according to the method reported by Tamura et al. with some modifications.[43] Fifteen prepared mycelial agar discs (4 mm) from a 7-day-old culture were inoculated in 100 mL of potato dextrose broth (potato infusion from 200 g/L, 20 g/L dextrose) with the EC_{50} (28.45 μg/mL) or EC_{70} (49.97 μg/mL) amount of carabrone and incubated at 25 °C and 180 rpm for 7 days in the dark. Mycelia were harvested by filtration with sterile gauze and washed three times using a 0.7% NaCl isotonic solution. After freeze-drying for 24 h, a certain quantity of mycelial cells was ground in liquid nitrogen, and the obtained powder was then resuspended in a 5-fold volume of the precooling extraction buffer (10 mM KCl, 5 mM EDTA, 250 mM sucrose, 1.5 mg/mL BSA, 20 mM HEPES−Tris pH 7.2) for homogenization. The homogenate was centrifuged (1500 rpm, 10 min, 4 °C), and the supernatant was retained. The precipitate obtained was resuspended in the same volume of extraction buffer and recentrifuged under the above conditions. The supernatant was combined and centrifuged at 4 °C (10 000 rpm, 20 min). The resulting precipitate was washed with the extraction buffer without BSA. The final mitochondrial fraction was suspended in a small volume of a cold buffer solution (250 mM sucrose, 20 mM HEPES−Tris, pH 7.2), resulting in the mitochondrial sample. All the experiments were performed in triplicate. The protein level of a mitochondrial sample was detected by the Coomassie Brilliant Blue G-250 dye binding method[44] and used as the marker of the mitochondrial concentration.[45]

Absorption Kinetics of TTY in Mycelial Cells. TTY was dissolved in an aqueous solution (0.2% DMSO) to prepare working solutions with different concentrations (0.3, 0.35, 0.4, and 0.8 μM).

Mycelial cells were inoculated in potato dextrose broth and cultivated in darkness at 25 °C on an Eberbach rotary shaker at 150 rpm for 72 h.

For the absorption kinetics study, the prepared mycelia were washed three times with ultrapure water, and then the surface water was removed using a filter paper. The mycelial cells (10 mg, wet weight) were placed on a glass slide and stained with the prepared solution of TTY (20 μL) in the dark at room temperature for a designated time period (5, 10, 15, 30, 60, 90, 120, 150, 180, 210, or 240 min). After being fully washed, the samples were observed with a structured illumination microscope (Observer Zl, Zeiss, Oberkochen, Germany) with the excitation wavelength at 365 nm and the emission wavelength at 445 nm. The sample not treated with TTY was used as the control. The fluorescence intensity per unit area of 90 hyphae in one visual field was counted by an ImageJ software package, and three visual fields were randomly selected for each treatment.

Stability of TTY in Mycelial Cells. Mycelial cells (500 mg, wet weight) were stained with a TTY working solution (1 mL, 0.4 μM) in the dark at room temperature for 90 min. After being stained, the mycelial cells were fully washed to remove the free TTY and then kept under the same conditions for another 2 h. The obtained mycelial cells were collected and ground in liquid nitrogen. The sample was then extracted with methanol (2 mL, chromatographic grade) and centrifuged at 4 °C (8000 rpm, 5 min). The supernatant was filtered by a Millipore filter (0.22 μm) for LC-HRMS analysis. Mycelial cells without the TTY treatment were used as the control. The LC-HRMS analysis was performed on an AB Sciex TripleTOF 5600+ System (Framingham, MA) using a methanol−water elution system (0−5 min, 10 vol % methanol in water; 5−10 min, 10 to 40% methanol; 10−15 min, 40 to 70% methanol; 15−20 min, 70 to 90% methanol; and 20−25 min, 90 to 100% methanol). A C_{18} reversed-phase column was used for the separation. The injection volume was 10 μL, and the flow rate was 1 mL/min.

Cell Imaging. Stocks of carabrone (0.1 mM), TTY (0.4 mM), MitoTrackerR Green FM (1 mM), and MitoTrackerR Red CMXRos (1 mM) were freshly prepared using DMSO as the solvent and diluted with ultrapure water before use. All the dyeing processes in this paper were operated under dark conditions. The Pearson's colocalization coefficient was calculated using a Colocalization Finder plugin of the free image-processing software ImageJ. The software and plugin are available on the ImageJ website (https://imagej.nih.gov/ij/).

For the FC imaging, mycelial cells (10 mg, wet weight) were washed three times with ultrapure water and then incubated with a mixture solution containing 0.4 μM TTY and 100 nM MitoTrackerR Green FM at room temperature for 1 h. After being rinsed with ultrapure water to remove the free dyes, the mycelial cells were redyed with RedDot1 (1:200 dilution) under constant conditions (30 °C, 1 h). After being fully washed, the sample was directly observed with a structured illumination microscope (Observer Zl, Zeiss, Oberkochen, Germany). TTY was excited at 365 nm and had an emission wavelength of 445 nm. The mitochondrial probe, MitoTrackerR Green FM, was excited at 470 nm and had an emission wavelength of 525 nm. The excitation of RedDot1 was carried out using 640 nm light, and the emission wavelength was 690 nm. Photos were collected using Axio Visio Release 4.8.2 SP3 software.

For the IF imaging, the prepared mycelial cells were first incubated with a carabrone solution (0.1 μM) at 25 °C for 12 h. Then, the sample was washed with ultrapure water three times to drain off the free carabrone. After being stained with MitoTrackerR Red CMXRos (100 nM) at 25 °C for 2 h, the mycelial cells were fixed with 2% paraformaldehyde for 40 min, and the fixed cells were rinsed three times with MSB (PIPES, 50 mM, EGTA, 2 mM, $MgSO_4$, 2 mM; pH 6.9) at 5 min intervals. The sample was then added to a mixed-enzyme solution (cellulase/Driselase/lyticase) for 5 min in the dark. After enzymolysis, the mycelial cells were washed with PBS (10 mM, pH 7.2) three times at 5 min intervals and blocked in PBS supplemented with BSA (5 mg/mL) for 30 min in the dark. The sample was stained successively with the primary antibody (1:1000 dilution in PBS, 37 °C, 1 h) and anti-mouse IgG (whole molecule)-FITC (1:100 dilution in PBS, 37 °C, 1 h) and washed with PBS as above following each staining period. After immunofluorescence staining, the sample

imaging was performed directly on a confocal laser-scanning microscope equipped with the Leica application suite advanced fluorescence software (Leica TCS SP8, Wetzlar, Germany). The excitation wavelength of MitoTrackerR Red CMXRos is 561 nm, and its emission spectrum is 630−660 nm. The excitation wavelength of anti-Mouse IgG (whole molecule)-FITC is 488 nm, and its emission spectrum is 520−550 nm.

■ RESULTS AND DISCUSSION

Synthesis and Characterization. *TTY.* For the fluorescence localization analysis, a fluorescent carabrone conjugate, TTY, was designed and synthesized according to the synthetic route illustrated in Scheme 1. N-Methyl anthranilic acid (TY) was chosen as the fluorogen, the carboxyl group of which was first activated by NSH to obtain N-methyl anthranilic acid succinimidyl ester (1).[35] Compound 1 was further modified by ethylenediamine to give N-(2-aminoethyl)-2-(methylamino)-benzamide (HH2).[36] Additionally, the carboxylated carabrone derivative, HH1, was prepared through the imidization of carabrone with carboxymethoxyamine hydrochloride using sodium acetate as the catalyst under a nitrogen atmosphere.[34] TTY was finally obtained through the condensation reaction between HH1 and HH2 in the presence of EDC as the coupling reagent and DMAP as the catalyst under mild conditions. The structures of the newly synthesized compounds were characterized correctly by ^{1}H NMR, ^{13}C NMR, and ESI-MS (Figures S1−S6). Moreover, a fluorescence spectrophotometer was also employed to investigate the fluorescent properties of compound TTY, with the results shown in Figure S7. TTY exhibited excitation- and emission-spectra maximum peaks at 381 nm ($\lambda_{\text{ex, max}}$) and 445 nm ($\lambda_{\text{em, max}}$) in methanol, respectively.

Hapten-Protein Conjugates. As outlined in Scheme 1, immunogen (T-BSA) was prepared by the active-ester method,[37] using HH1 as the hapten and BSA as the carrier for polyclonal antibody production. Additionally, the coating antigen (T-OVA) was synthesized through the coupling of HH1 with OVA by the mixed-anhydride method[38] for indirect ELISAs. SDS-PAGE was used for mobility-shift detection of the hapten-protein conjugates, and the results were shown in Figure S8. From the SDS-PAGE, the bands of T-BSA and T-OVA appeared at higher molecular-weight positions with slower mobilities relative to their unreacted proteins, indicating successful protein conjugation.

The ultraviolet−visible spectral changes of the hapten-protein conjugates were also monitored to confirm their identities by UV spectroscopy. As shown in Figure S9, T-BSA exhibited a 10 nm blue shift from 278 to 268 nm relative to BSA, and T-OVA exhibited a 7 nm blue shift from 278 to 270 nm relative to OVA under the same conditions, verifying that HH1 was successfully attached to the carrier proteins.

Production of the Polyclonal Antibody. Antigen design plays a key role in polyclonal-antibody production. Because of the weak antigenicity of carabrone, which has a low molecular weight, it must be coupled to a carrier protein to elicit an immune response.[46] In order to generate an antibody with high sensitivity and specificity, the binding strategy was designed cautiously to ensure that there were minimal conformational changes in hapten relative to the targeted analyte even after its conjugation with the carrier protein.[47] Moreover, previous study revealed that antibodies produced by single antigens might have higher affinities to their targets.[37] On the basis of this information, HH1, which retained the core structure of

carabrone, was selected as the hapten, and its BSA conjugate was selected as the immunogen. After four rounds of immunization with single T-BSA, polyclonal antisera produced by six female BALB/c mice were isolated, and their titers against carabrone were tested by indirect ELISAs (Table S1). The antisera (TPAbs-1−6) exhibited different affinities to the coating antigen (T-OVA) with titers ranging from 64 000 to 256 000, which were higher than those of previously reported antisera against various pesticides.[48] TPAbs-4, which had the highest titer (256 000), was selected for antibody purification. The concentration of the purified polyclonal antibody was about 4.52 mg/mL.

Antifungal Activity. The physicochemical properties of a parent compound, including the molecular weight and the octanol/water partitioning coefficient value, will inevitably be changed if it is modified with a fluorogen, which may even consequently affect its combination with its target. Previous studies from our group showed that carabrone derivatives modified at their C-4 positions exhibited diverse antifungal activities against *Botrytis cinereal* and *Colletotrichum lagenarium*, which were the results of the altering of their affinities to the unclear target of carabrone.[49,50] Thus, to investigate the effect of a substituent fluorogen on carabrone's recognition of its target, the effects of TTY and carabrone on the mycelial growth of Ggt were evaluated in vitro. As illustrated in Table 1, TTY

Table 1. Antifungal Activity of Carabrone and TTY against Ggt

compounds	$EC_{50}{}^a$ (μg/mL)	slope ± SE	$CI_{95}{}^b$	Chi^c
carabrone	28.45	2.15 ± 0.24	25.07−29.01	0.23
TTY	33.68	3.35 ± 0.12	29.14−35.45	0.16

^{a}Effective dose for 50% inhibition compared with the growth of the control. ^{b}Confidence intervals of 95%. ^{c}Chi-square value, significant at $P < 0.05$ level.

had a similar EC_{50} value (33.68 μg/mL) to that of carabrone (28.45 μg/mL), verifying that TTY still maintains the capacity to selectively bind to the target of carabrone. Thus, the fluorescent conjugate (TY) does not affect the biological activity of carabrone.

Absorption Kinetics of TTY. To determine the potential of TTY to be used as a fluorescent subcellular tracer, the absorption behavior of TTY was examined by monitoring the fluorescence intensity of mycelia stained with different concentrations of TTY (0.3, 0.35, 0.4, and 0.8 μM) over various time periods (0−240 min). As depicted in Figure 2, TTY absorption exhibited time- and dose-dependent behavior. Adsorption equilibrium was reached after 90 min, and absorption saturation was reached when the concentration of TTY was over 0.4 μM. We thus used the optimized staining condition (0.4 μM TTY, dyeing time of 90 min) for the localization experiment. Under the obtained optimal conditions, a fluorescence image with evident subcellular distribution was obtained (Figure S10), which indicated that TTY could enter the mycelial cells of Ggt for cell imaging.

Stability of TTY in Mycelial Cells. An ideal fluorescent tracer should be stable throughout the imaging period. Thus, the presence of TTY in the mycelial cells at 2 h was identified by LC-HRMS analysis. As shown in Figure S11, the chromatographic peak for compound TTY (m/z, $[M + H]^+$ 497.2751 and $[M + Na]^+$ 519.2583) was found at 14.18 min while no identical chromatographic peak of TTY was found in
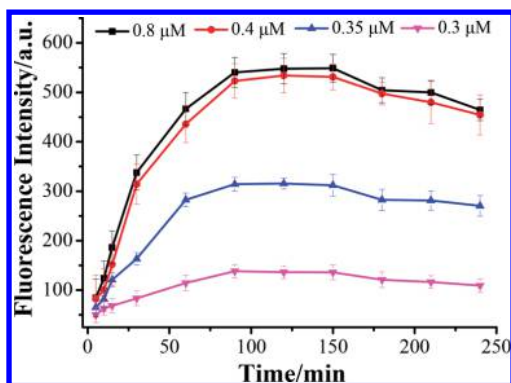
Figure 2. Fluorescence changes of mycelial cells stained with different concentrations of TTY (0.3, 0.35, 0.4, and 0.8 μM) for various time periods.

the control group (Figure S12). Moreover, we searched for the possible decomposition products of TTY (Figure S14) in the TOF-MS spectrum from 6 to 25 min using the Analyst TF 1.7.1 Software, and there were no matching MS peaks for those products (Figure S13). Therefore, TTY was relatively stable during the experimental period. These findings indicate that TTY is a suitable fluorescent surrogate of carabrone and is believed to be capable of revealing the subcellular localization of carabrone within Ggt.

Hyphal Morphology and Ultrastructure. Previous work of our group showed that carabrone possessed a remarkable inhibitory effect against the mycelial growth of Ggt.[17] To gain more evidence about the mode of antifungal action of carabrone treatment, the hyphal morphology of Ggt was observed by SEM, with the results shown in Figure 3. The control sample exhibited the normal morphology of uniform, smooth, uniseriate, and robust hyphae with plump growing points (Figure 3a). The carabrone treated sample, however, showed altered morphology characterized by twisted and irregular hyphae with slight deformities at the growing points (Figure 3b) and even cellular collapse (Figure 3c).

TEM was employed to study the ultrastructural alterations of Ggt when treated with carabrone, and the results were illustrated in Figure 4. A typical fungal ultrastructure of intact cell walls with normal thicknesses, regular and smooth cell membranes, evenly distributed cellular cytoplasm, and regularly shaped organelles is clearly represented by the TEM images of the mycelia the control treatment (Figure 4a,b). For the mycelia treated with the EC_{50} amount of carabrone, no evident changes were viewed in the structures of the cell walls, cell membranes, or diaphragms of the mycelia. Interestingly, mitochondrial abnormalities were observed in the treated mycelia, which could be described as (i) mitochondria having

hazy outlines (Figure 4c), (ii) a medullary transition in mitochondria (Figure 4d), (iii) an excess accumulation of unclear settlings in mitochondria (Figure 4e), and (iv) vacuolar degeneration of mitochondria (Figure 4f). These findings suggested that the mitochondria of Ggt might correlate with the action mechanism of carabrone.

Mitochondrial Concentration. To validate our ultrastructural findings, we sought to test the changes in mitochondrial concentration of Ggt treated with carabrone. The effect of carabrone on mitochondrial concentration was evaluated by testing the protein contents of the mitochondria (Table 2).[45] After exposure to carabrone for 7 days, the mitochondrial concentration of Ggt decreased evidently ($P <$ 0.05) along with an increasing concentration of carabrone (EC_{50}, 28.45 μg/mL; EC_{70}, 49.97 μg/mL), in agreement with the alterations of mitochondrial structure.

Subcellular Imaging. Given the fact that the aforementioned effects of carabrone on Ggt (e.g., the ultrastructural alterations and decreases in mitochondrial concentration) are closely related to mitochondria, two imaging techniques (FC and IF) were employed to validate the mitochondrial targeting of carabrone.

For the FC imaging, three dyes with distinctive emission wavelengths (TTY, 445 nm; MitoTrackerR Green FM, 525 nm; and RedDot1, 690 nm) were utilized. As depicted in Figures 5 and S15, TTY and MitoTrackerR Green FM (a mitochondrial dye) overlapped perfectly, whereas no overlay was observed between TTY and RedDot (a commercial nuclear probe). Pearson's colocalization coefficient,[51,52] which described the correlation of the intensity distributions of the TTY and MitoTrackerR Green FM signals, was 0.83 (Figure 5h). Thus, FC imaging strongly supports the mitochondrial localization of carabrone.

For the IF imaging, a polyclonal antibody specific to carabrone was used as the primary antibody to recognize intracellular carabrone, and FITC-labeled anti-mouse IgG (whole molecule) was used as the secondary antibody. A commercially available dye, MitoTrackerR Red CMXRos, was employed for this colocalization study. Again, excellent colocalization between anti-mouse IgG (whole molecule)-FITC and MitoTrackerR Red CMXRos was observed (Figures 6 and S16), with the Pearson's colocalization coefficient being 0.86 (Figure 6f). These results suggested that carabrone was predominantly present in the mitochondria.

α,β-Unsaturated lactones, such as britannin,[20] arucanolide,[21] parthenolide,[22] costunolide,[23] and isocostunolide[24] exert their biologic functions via mitochondria-related pathways. Our previous study showed that carabrone could inhibit intracellular oxidation processes in Ggt and exert some impacts on mitochondria, such as vacuolar degeneration,[25] which was
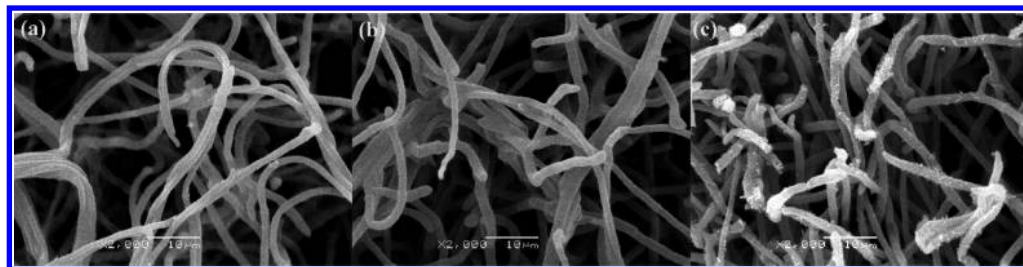

Figure 3. Scanning-electron-microscope images of the hyphal morphology of Ggt. (a) Healthy hyphae in control Petri plates. (b,c) Hyphae treated with carabrone (28.45 μg/mL) for 7 days. Scale bar: 10 μm.
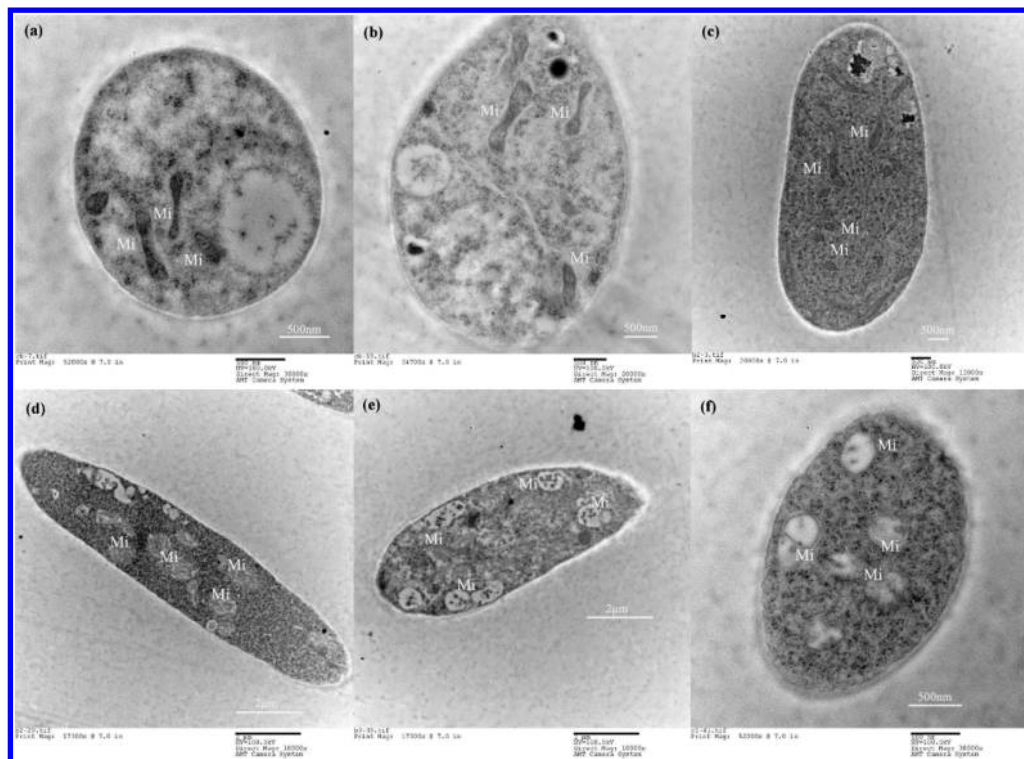
Figure 4. Transmission-electron-microscopic images of hyphal ultrastructures of Ggt. (a,b) Healthy hyphae in control Petri plates. (c−f) Hyphae treated with carabrone (28.45 μg/mL) for 7 days. Mi: mitochondria. Scale bar: 500 nm (a−c,f) or 2 μm (d−e).

Table 2. Mitochondrial Concentration of Ggt Treated with Carabrone for 7 Days

carabrone (μg/mL)	mitochondrial concentration[a] (mg/mL)
0	1.61 ± 0.024 a
28.45	1.15 ± 0.047 b
49.97	0.97 ± 0.072 c

[a]The data of were the averages of three repetitions. Significant differences were at $P < 0.01$ by Duncan's multiple-range test.

consistent with the results obtained in this study. Additionally, when treated with carabrone, the activities of respiratory chain complexes I−V were determined to be significantly decreased, especially that of the complex III, and the expression levels of the associated genes, except *GgCyc1*, were upregulated,[26] demonstrating that carabrone was involved in the respiratory electron-transfer pathway either directly or indirectly in Ggt. In this paper, we confirmed not only the effects of carabrone on mitochondrial structure and concentration but also its mitochondrial targeting using FC and IF imaging techniques.
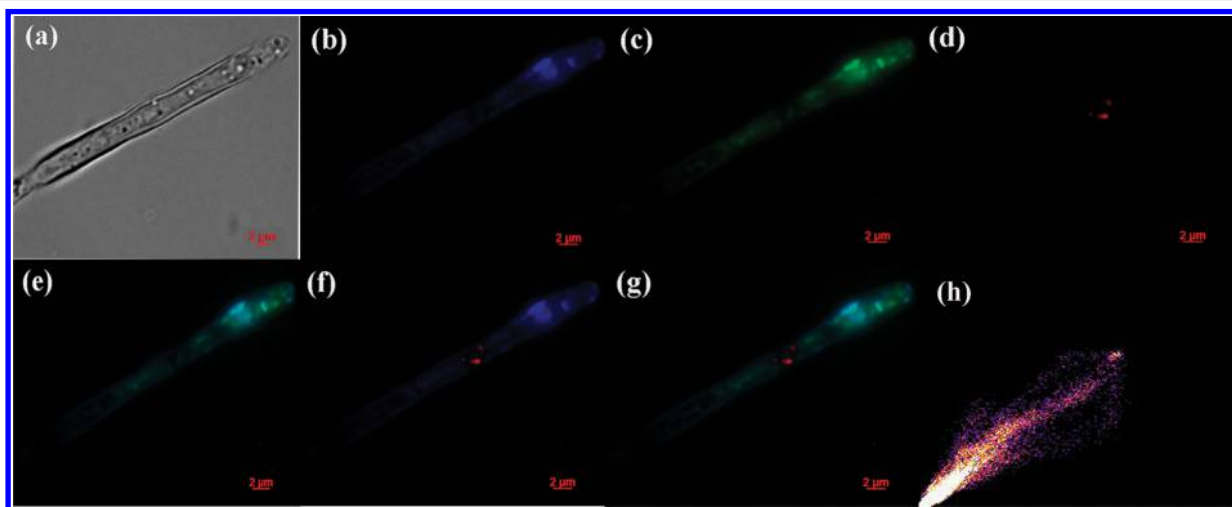

Figure 5. Fluorescence images of hyphae costained with TTY, MitoTrackerR Green FM, and RedDot. (a) Bright-field image of the mycelial cells in the sample. (b) Image of TTY (emission wavelength, 445 nm). (c) Image of MitoTrackerR Green FM (emission wavelength, 525 nm). (d) Image of RedDot (emission wavelength, 690 nm). (e) Overlay of the TTY and MitoTrackerR Green FM images (b,c). (f) Overlay of the TTY and RedDot images (b,d). (g) Overlay of the TTY, MitoTrackerR Green FM, and RedDot images (b−d). (h) Colocalization profile of TTY and MitoTrackerR Green FM. Scale bar: 2 μm. Magnification: 100×.
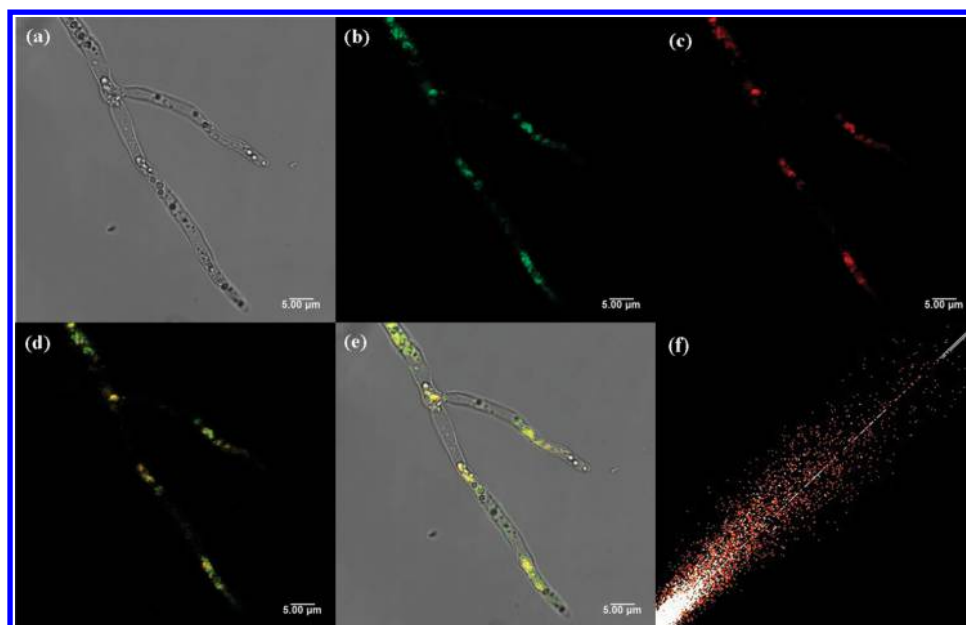
Figure 6. Confocal immunofluorescence images of hyphae treated with carabrone and costained with anti-mouse IgG (whole molecule)-FITC and MitoTrackerR Red CMXRos. (a) Bright-field image of the hyphae. (b) Image of anti-mouse IgG (whole molecule)-FITC (green emission, 520−550 nm). (c) Image of MitoTrackerR Red CMXRos (red emission, 630−660 nm). (d) Overlay of the anti-mouse IgG (whole molecule)-FITC and MitoTrackerR Red CMXRos images (b,c). (e) Overlay of the bright-field, anti-mouse IgG (whole molecule)-FITC, and MitoTrackerR Red CMXRos images (a−c). (f) Colocalization profile of anti-mouse IgG (whole molecule)-FITC and MitoTrackerR Green FM. Scale bar: 5 μm. Magnification: 60×.

An excessive accumulation of reactive oxygen species (ROS) in mitochondria was also observed in Ggt treated with carabrone (data not published). These results indicate that carabrone selectively distributes in the mitochondria of Ggt and functions on the respiratory electron-transport chain, especially on complex III, which leads to ROS increase and death of the mycelial cells. However, the detailed pathway of carabrone's action on mitochondria is still unclear, and further study of the mitochondria-related pathway induced by carabrone in Ggt is in progress.

In conclusion, the major effects of carabrone as a potential botanical antifungal agent against Ggt were the variations in mitochondrial structure and the decreased concentration of mitochondria. A fluorescent conjugate of carabrone, TTY, was well designed and first obtained via covalent coupling of a smart fluorophore with a soft linker. Its antifungal activity and absorption kinetics indicated that TTY was a reasonable fluorescent surrogate of carabrone and suitable to reveal the subcellular distribution of carabrone analogues. A polyclonal antibody specific to carabrone was also successfully prepared by immunizing mice with a well-designed immunogen according to a standard protocol. Subcellular imaging with FC and IF provided identical and adequate evidence that the actual site of action of carabrone lay in the mitochondria of Ggt, orienting our follow-up study on the elucidation of the detailed mechanism of carabrone against Ggt. More importantly, the strategies established for the subcellular-localization study of a natural substance in this paper could be also applied in exploring the action mechanism of other drugs.

■ ASSOCIATED CONTENT

Ⓢ Supporting Information

The Supporting Information is available free of charge on the ACS Publications website at DOI: 10.1021/acs.jafc.7b03913.

^{1}H NMR, ^{13}C NMR, and MS spectra; excitation and emission spectra of TTY; SDS-PAGE; UV spectra; antiserum titers; fluorescence image of mycelial cells stained with TTY; LC-HRMS spectra; possible decomposition products of TTY; FC imaging; IF imaging (PDF)

■ AUTHOR INFORMATION

Corresponding Author

*Fax: +86-029-87092122, E-mail: fengjt@nwafu.edu.cn.

ORCID Ⓘ

Juntao Feng: 0000-0002-5320-1178

Notes

The authors declare no competing financial interest.

■ REFERENCES

(1) Gutteridge, R. J.; Bateman, G. L.; Todd, A. D. Variation in the effects of take-all disease on grain yield and quality of winter cereals in field experiments. *Pest Manage. Sci.* **2003**, *59*, 215−224.

(2) Keenan, S.; Cromey, M.; Harrow, S.; Bithell, S.; Butler, R.; Beard, S.; Pitman, A. Quantitative PCR to detect *Gaeumannomyces graminis* var. *tritici* in symptomatic and non-symptomatic wheat roots. *Australas. Plant Pathol.* **2015**, *44*, 591−597.

(3) Yang, M. M.; Mavrodi, D. V.; Mavrodi, O. V.; Bonsall, R. F.; Parejko, J. A.; Paulitz, T. C.; Thomashow, L. S.; Yang, H. T.; Weller, D. M.; Guo, J. H. Biological control of take-all by fluorescent *Pseudomonas spp.* from Chinese wheat fields. *Phytopathology* **2011**, *101*, 1481−1491.

(4) Kwak, Y.-S.; Bakker, P. A.; Glandorf, D. C.; Rice, J. T.; Paulitz, T. C.; Weller, D. M. Diversity, virulence, and 2, 4-diacetylphloroglucinol sensitivity of *Gaeumannomyces graminis* var. *tritici* isolates from Washington State. *Phytopathology* **2009**, *99*, 472−479.

(5) Lei, P.; Zhang, X. B.; Xu, Y.; Xu, G. F.; Liu, X. L.; Yang, X. L.; Zhang, X.; Ling, Y. Synthesis and fungicidal activity of pyrazole derivatives containing 1, 2, 3, 4-tetrahydroquinoline. *Chem. Cent. J.* **2016**, *10*, 40.

(6) Pérez-García, A.; Romero, D.; De Vicente, A. Plant protection and growth stimulation by microorganisms: biotechnological applications of *Bacilli* in agriculture. *Curr. Opin. Biotechnol.* **2011**, *22*, 187−193.

(7) Yoon, M. Y.; Cha, B.; Kim, J. C. Recent trends in studies on botanical fungicides in agriculture. *Plant Pathol. J.* **2013**, *29*, 1−9.

(8) Cook, R. J. Take-all of wheat. *Physiol. Mol. Plant Pathol.* **2003**, *62*, 73−86.

(9) Kwak, Y. S.; Weller, D. M. Take-all of wheat and natural disease suppression: a review. *Plant Pathol. J.* **2013**, *29*, 125.

(10) Liu, B.; Qiao, H. P.; Huang, L. L.; Buchenauer, H.; Han, Q. M.; Kang, Z. S.; Gong, Y. F. Biological control of Take-all in wheat by endophytic *Bacillus Subtilis* E1r-J and potential mode of action. *Biol. Control* **2009**, *49*, 277−285.

(11) Yang, L. R.; Quan, X.; Xue, B. G.; Goodwin, P. H.; Lu, S. B.; Wang, J. H.; Du, W.; Wu, C. Isolation and identification of *Bacillus subtilis* strain YB-05 and its antifungal substances showing antagonism against *Gaeumannomyces graminis* var. *Biol. Control* **2015**, *85*, 52−58.

(12) Gong, L.; Tan, H. B.; Chen, F.; Li, T. T.; Zhu, J. Y.; Jian, Q. J.; Yuan, D. B.; Xu, L. X.; Hu, W. Z.; Jiang, Y. M.; Duan, X. W. Novel synthesized 2, 4−DAPG analogues: antifungal activity, mechanism and toxicology. *Sci. Rep.* **2016**, *6*, 32266 DOI: 10.1038/srep32266.

(13) Feng, J. T.; Ma, Z. Q.; Li, J. H.; He, J.; Xu, H.; Zhang, X. Synthesis and antifungal activity of carabrone derivatives. *Molecules* **2010**, *15*, 6485−6492.

(14) Maruyama, M.; Omura, S. Carpesiolin from *Carpesium abrotanoides*. *Phytochemistry* **1977**, *16*, 782−783.

(15) Yang, C.; Shi, Y. P.; Jia, Z. J. Sesquiterpene lactone glycosides, eudesmanolides, and other constituents from. *Planta Med.* **2002**, *68*, 626−630.

(16) Jiang, J. W. *Manuscript of Active Ingredients of Vegetable Drug*. *People's Health Press Beijing, China* **1986**.

(17) Han, X. S.; Xu, D.; Feng, J. T.; Zhang, X. Fungicidal activity of carabrone. *J. Northwest A&F Univ.* **2014**, *42*, 178−184.

(18) Zhang, S. Y.; Won, Y. K.; Ong, C. N.; Shen, H. M. Anti-cancer potential of sesquiterpene lactones: bioactivity and molecular mechanisms. *Curr. Med. Chem.: Anti-Cancer Agents* **2005**, *5*, 239−249.

(19) Kitson, R. R.; Millemaggi, A.; Taylor, R. J. The Renaissance of α-Methylene-γ-butyrolactones: New Synthetic Approaches. *Angew. Chem., Int. Ed.* **2009**, *48*, 9426−9451.

(20) Hamzeloo-Moghadam, M.; Aghaei, M.; Fallahian, F.; Jafari, S. M.; Dolati, M.; Abdolmohammadi, M. H.; Hajiahmadi, S.; Esmaeili, S. Britannin, a sesquiterpene lactone, inhibits proliferation and induces apoptosis through the mitochondrial signaling pathway in human breast cancer cells. *Tumor Biol.* **2015**, *36*, 1191−1198.

(21) Nakagawa, Y.; Iinuma, M.; Matsuura, N.; Yi, K.; Naoi, M.; Nakayama, T.; Nozawa, Y.; Akao, Y. A potent apoptosis-inducing activity of a sesquiterpene lactone, arucanolide, in HL60 cells: a crucial role of apoptosis-inducing factor. *J. Pharmacol. Sci.* **2005**, *97*, 242.

(22) Zhang, S.; Ong, C. N.; Shen, H. M. Involvement of proapoptotic Bcl-2 family members in parthenolide-induced mitochondrial dysfunction and apoptosis. *Cancer Lett.* **2004**, *211*, 175−188.

(23) Lee, M.-G.; Lee, K.-T.; Chi, S.-G.; PARK, J.-H. Costunolide induces apoptosis by ROS-mediated mitochondrial permeability transition and cytochrome C release. *Biol. Pharm. Bull.* **2001**, *24*, 303−306.

(24) Chen, C. N.; Huang, H. H.; Wu, C. L.; Lin, C. P.; Hsu, J. T.; Hsieh, H. P.; Chuang, S. E.; Lai, G. M. Isocostunolide, a sesquiterpene lactone, induces mitochondrial membrane depolarization and caspase-dependent apoptosis in human melanoma cells. *Cancer Lett.* **2007**, *246*, 237.

(25) Wang, Y. M. *Effects of carabrone on five plant diseases and the growth and development of Gaeumannomyces graminis var. tritici*; Northwest A&F University: Yangling, 2009.

(26) Wang, M.; Wang, L. Y.; Han, L. R.; Zhang, X.; Feng, J. T. The effect of carabrone on mitochondrial respiratory chain complexes in Gaeumannomyces Graminis. *J. Appl. Microbiol.* **2017**, *123*, 1100−1110.

(27) Stadler, C.; Rexhepaj, E.; Singan, V. R.; Murphy, R. F.; Pepperkok, R.; Uhlén, M.; Simpson, J. C.; Lundberg, E. Immunofluorescence and fluorescent-protein tagging show high correlation for protein localization in mammalian cells. *Nat. Methods* **2013**, *10*, 315−323.

(28) Gonzalez, A. A.; Prieto, M. C. Roles of collecting duct renin and (pro) renin receptor in hypertension: mini review. *Ther. Adv. Cardiovasc. Dis.* **2015**, *9*, 191−200.

(29) Thurber, G. M.; Yang, K. S.; Reiner, T.; Kohler, R. H.; Sorger, P.; Mitchison, T.; Weissleder, R. Single-cell and subcellular pharmacokinetic imaging allows insight into drug action in vivo. *Nat. Commun.* **2013**, *4*, 1504.

(30) Vinegoni, C.; Dubach, J. M.; Thurber, G. M.; Miller, M. A.; Mazitschek, R.; Weissleder, R. Advances in measuring single-cell pharmacology in vivo. *Drug Discovery Today* **2015**, *20*, 1087−1092.

(31) Irani, N. G.; Di Rubbo, S.; Mylle, E.; Van den Begin, J.; Schneider-Pizoń, J.; Hniliková, J.; Šíša, M.; Buyst, D.; Vilarrasa-Blasi, J.; Szatmári, A.-M.; Van Damme, D.; Mishev, K.; Codreanu, M.-C.; Kohout, L.; Strnad, M.; Caño-Delgado, A. I.; Friml, J.; Madder, A.; Russinova, E. Fluorescent castasterone reveals BRI1 signaling from the plasma membrane. *Nat. Chem. Biol.* **2012**, *8*, 583−589.

(32) Wang, J.; Lei, Z. W.; Wen, Y. J.; Mao, G. L.; Wu, H. X.; Xu, H. H. A novel fluorescent conjugate applicable to visualize the translocation of glucose-fipronil. *J. Agric. Food Chem.* **2014**, *62*, 8791−8798.

(33) Kang, C. K.; Yamada, K.; Usuki, Y.; Ogita, A.; Fujita, K. I.; Tanaka, T. Visualization analysis of the vacuole-targeting fungicidal activity of amphotericin B against the parent strain and an ergosterol-less mutant of Saccharomyces cerevisiae. *Microbiology* **2013**, *159*, 939−947.

(34) Boivin, J.; Fouquet, E.; Schiano, A. M.; Zard, S. Z. Iminyl radicals: Part III. Further synthetically useful sources of iminyl radicals. *Tetrahedron* **1994**, *50*, 1769−1776.

(35) Gavande, N.; Kim, H. L.; Doddareddy, M.; Johnston, G. A. R.; Chebib, M.; Hanrahan, J. R. Design, Synthesis, and Pharmacological Evaluationof Fluorescent and Biotinylated Antagonists of ρ1 GABAC Receptors. *ACS Med. Chem. Lett.* **2013**, *4*, 402−407.

(36) Leung, A. H.; Jin, J. F.; Wang, S. X.; Lei, H.; Wong, W. T. Inflammation targeted Gd(3+)-based MRI contrast agents imaging tumor and rheumatoid arthritis models. *Bioconjugate Chem.* **2014**, *25*, 1112−1123.

(37) Shi, H. Y.; Li, H. X.; Hua, X. D.; Zheng, Z. T.; Zhu, G. N.; Wang, M. H. Characterization of Multihapten Antigens on Antibody Sensitivity and Specificity for Parathion. *Anal. Lett.* **2014**, *47*, 2699−2707.

(38) Gendloff, E. H.; Casale, W. L.; Ram, B. P.; Tai, J. H.; Pestka, J. J.; Hart, L. P. Hapten-protein conjugates prepared by the mixed anhydride method: Cross-reactive antibodies in heterologous antisera. *J. Immunol. Methods* **1986**, *92*, 15.

(39) Leenaars, M.; Hendriksen, C. F. Critical steps in the production of polyclonal and monoclonal antibodies: evaluation and recommendations. *ILAR J.* **2005**, *46*, 269−279.

(40) Manclús, J. J.; Montoya, A. Development of immunoassays for the analysis of chlorpyrifos and its major metabolite 3,5,6-trichloro-2-pyridinol in the aquatic environment. *Anal. Chim. Acta* **1995**, *311*, 341−348.

(41) Rios, J. L.; Recio, M. C.; Villar, A. Screening methods for natural products with antimicrobial activity: A review of the literature. *J. Ethnopharmacol.* **1988**, *23*, 127−149.

(42) Shao, X.; Cheng, S.; Wang, H.; Yu, D.; Mungai, C. The possible mechanism of antifungal action of tea tree oil on Botrytis cinerea. *J. Appl. Microbiol.* **2013**, *114*, 1642−1649.

(43) Tamura, H.; Mizutani, A.; Yukioka, H.; Miki, N.; Ohba, K.; Masuko, M. Effect of the methoxyiminoacetamide fungicide, SSF129, on respiratory activity in. *Pestic. Sci.* **1999**, *55*, 681−686.

(44) Grintzalis, K.; Georgiou, C. D.; Schneider, Y. J. An accurate and sensitive Coomassie Brilliant Blue G-250-based assay for protein determination. *Anal. Biochem.* **2015**, *480*, 28−30.

(45) Frezza, C.; Cipolat, S.; Scorrano, L. Organelle isolation: functional mitochondria from mouse liver, muscle and cultured fibroblasts. *Nat. Protoc.* **2007**, *2*, 287.

(46) Hertzog, P. J.; Shaw, A.; Smith, J. R. L.; Garner, R. C. Improved conditions for the production of monoclonal antibodies to carcinogen-modified DNA, for use in enzyme-linked immunosorbent assays (ELISA). *J. Immunol. Methods* **1983**, *62*, 49−58.

(47) Spinks, C. A. Broad-specificity immunoassay of low molecular weight food contaminants: new paths to Utopia. *Trends Food Sci. Technol.* **2000**, *11*, 210−217.

(48) Liu, R.; Liu, Y.; Lan, M. J.; Taheri, N.; Cheng, J. L.; Guo, Y. R.; Zhu, G. N. Evaluation of a water-soluble adjuvant for the development of monoclonal antibodies against small-molecule compounds. *J. Zhejiang Univ., Sci., B* **2016**, *17*, 282−293.

(49) Feng, J. T.; Wang, H.; Ren, S. X.; He, J.; Liu, Y.; Zhang, X. Synthesis and antifungal activities of carabrol ester derivatives. *J. Agric. Food Chem.* **2012**, *60*, 3817−3823.

(50) Wang, H.; Ren, S. X.; He, Z. Y.; Wang, D. L.; Yan, X. N.; Feng, J. T.; Zhang, X. Synthesis, antifungal activities and qualitative structure activity relationship of carabrone hydrazone derivatives as potential antifungal agents. *Int. J. Mol. Sci.* **2014**, *15*, 4257−4272.

(51) Yu, T. T.; Tian, X. H.; Li, H.; Li, W.; Zhu, W. J.; Zhou, H. P.; Tian, Y. P.; Wu, J. A reversible and highly selective fluorescence "on-off-on" probe for detecting nickel ion in the mitochondria of living cells. *Biosens. Bioelectron.* **2016**, *82*, 93−98.

(52) Manders, E. M.; Stap, J.; Brakenhoff, G. J.; van Driel, R.; Aten, J. A. Dynamics of three-dimensional replication patterns during the S-phase, analysed by double labelling of DNA and confocal microscopy. *J. Cell Sci.* **1992**, *103*, 857.